Automated Diagnosis of Malaria in Tropical Areas Using 40X Microscopic Images of Blood Smears

Kanaa Thomas F. N. *t_kanaa@yahoo.fr*
Higher Technical Teacher Training College / Department of Computer Sciences
University of Bamenda
Bamenda, P.O Box 39 Bambili, Cameroon

Laboratory of Electronics, Electrotechnics, Automation and Telecommunications
University of Douala
Douala, P.O Box 1872 Douala, Cameroon

Tchiotsop Daniel *dtchiot@yahoo.fr*
Fotso Victor University Institute of Technology
Laboratory of Automation and Applied Computer Science
University of Dschang
Bafoussam, P.O Box 134 Bandjoun, Cameroon

Ele Pierre *pierre_ele@yahoo.fr*
Laboratory of Electronics, Electrotechnics, Automation and Telecommunications
University of Douala
Douala, P.O Box 1872 Douala, Cameroon

Tonye Emmanuel *tonyee@hotmail.com*
National Advanced School of Engineering
Laboratory of Electronics and Signal Processing
University of Yaounde I
Yaoundé, P.O Box 8390 Yaoundé, Cameroon

Belong Philippe *phbel52@yahoo.fr*
Higher Teacher Training College / Department of Biological Sciences
University of Yaounde I
Yaoundé, P.O Box 47 Yaoundé, Cameroon

Abstract

This paper proposes a new algorithm to measure parasitemia stemming from *Plasmodium falciparum* by using optical images of capillary blood smears from Sub-Saharan Africa. The approach is an improvement of the previous noteworthy method by developing a two-tone adaptive median filter and Sauvola segmentation. The analysis was performed on the database of 100X and 40X microscopic images originating from real time collection of patients' blood of some Cameroon's laboratories. The obtained results were very satisfactory with a detection of infected cells on 40X images of a sensitivity at 81.58%, a specificity at 97.11% and an accuracy at 96.71%. Compared to the previous works, the values portray a real improvement in most performance's criteria for 100X images and 40X images as well. There is a significant step of automated Malaria diagnosis in tropical areas and in the performance assessed. The results of the method gave more strength for the two magnification ranges. The time spent in analysis is obviously reduced with 40X magnification and the inaccessibility of the information by the visual laboratory measurement is henceforth genuinely assaulted. The low cost of the system opens therefore the possibility of a cost effective method of diagnosing malaria in low and middle-income countries.

Keywords: Malaria, Plasmodium Falciparum, Median Filter, Sauvola Thresholding, Microscopic Imagery.

1. INTRODUCTION

Malaria is an endemic disease which is a leading cause of morbidity and mortality in tropical and sub-tropical countries. It is a mosquito-borne infectious disease of humans and other animals. In humans, it is caused by *Plasmodium falciparum, vivax, malariae* and *ovale* [1,2]. The most prevalent type in our context is the *P. falciparum* which is really a threat to health [3]. A significant part of literature expands on the subject, turning it to be so current and of high priority [4,5,6,7]. An estimated 207 million cases and 627 thousands malaria deaths are estimated to have occurred in 2012 [8]. The estimation of disease burden in Cameroon is 30 - 35% and 40 - 45% in the total deaths and morbidity cases respectively [9]. There is an urgent need to increase funding for malaria control and to expand program coverage, in order to meet international targets for reducing malaria cases and deaths [8]. In the exercise of diagnosing malaria reserved as the cornerstone of *WHO's initiative T3* (Test, Treat and Track), we focused our attention on the improvement of the first step. Diagnosis of malaria can be achieved using a number of different methods as Quantitative Buffy Coat (QBC), automated detection of Malaria pigment and image processing techniques.

In QBC method, nuclear material is stained using acridine orange which highlights white blood cells and parasites, and they can then be identified using UV light [10,11]. Though achieving a sensitivity of 75% and a specificity of 84%, the major problems of this technique are the cost of fluorescent microscopes, the capillary tubes [12,13] as well as the availability of acridine orange as it is considered hazardous [14]. To improve diagnosis, the detection of stained specific pigments was performed. An automated process using analyzers, programs flow cytometry, depolarized laser light and Volume Conductivity [15], was investigated. For 90% in sensitivity and 88% in specificity [16], the method improved from the previous but its required automated analysis is not available in most endemic regions.

Automated Malaria diagnosis based on Giemsa and Fristain stained blood smear images have also been addressed in several works using different approaches. A substantial literature review is presented in the works of Razzak [17] with the outline of some performance criteria in the recent developments for malarial parasite identification. Savkare et al. [18] implemented the image smoothening and edge sharpening with the median and Laplacian filters. Isolating the foreground from the background with Otsu thresholding, they used the distance transform and the watershed algorithm as tools of Red Blood Cells (RBC) segmentation. The subsequent deployment of the support vector machine (SVM) for cell classification permitted to obtain a sensitivity of 93.12% and a specificity of 93.17%.

For a global accuracy of the system at 97.73% in diagnosing malaria from Human RBC, Pranati et al. [19] exploited Sobel edge followed by Harris corner detection to identify malarial parasites. Even if performance criteria are becoming more and more interesting, the tools and techniques are not overemphasized on the improvement of execution time.

Rapid malaria diagnosis proposed by Maitethia [20] proceeds by means of median filter to reduce noise, the Otsu thresholding for the segmentation of cells and Zack thresholding for parasite segmentation. The cell and stage classification based on texture and color features are obtained through the Artificial Neural Network (ANN) for a result of sensitivity at 92% and specificity at 97%.

Still in the aim of accelerating the diagnosis, Imroze et al. [21] deployed an image processing method and compared it to his Plasmo-vision technique. The image processing develops an algorithm combining the Median filter, the Smallest Unit value Segment Assimilating Nucleus (SUSAN), with the Canny Edge detector and the Otsu global thresholding based on variances. For the segmentation, the marker controlled watershed, Top-Hat and Bottom-Hat Transform were implemented. The final classification of an erythrocyte and the species of the parasite through a two-stage binary tree-classifier on first order and moment invariant features helped to achieve a sensitivity of 90% and Predictive Positive Value of 80%.

Pramit et al. [22], to achieve an accuracy of 91.125%, rather used the Laplacian filtered separately on Red, Green and Blue components of the color images before the cell segmentation with an appropriate threshold. The comparison of two sets of binary images reveals or absence of *Plasmodium*.

In Aggraini's works [23], the median filter and global thresholding are used to remove noise and extract blood cells. The Bayes decision theory is then implemented on separate set of futures to build a two stage erythrocyte classifier based respectively on range intensity and ratio of white/black feature. The method performed a sensitivity of 92.59% and as a specificity of 99.65%, encouraging to classify the parasites by using its shape and size.

A counting of Red and White Blood Cells method with an accuracy of 94.58% by Pooja et al. [24] is developed from a database of 75 blood smears images. Essentially using the standard median filtering, the global thresholding and finally the blood cell factor estimation through the dilation of blood, the depth of the counting chamber and the small squares' number and area. Reinforced in accuracy with 0.06% by Pawan et al. [25] with the segmentation and the edge detection through the Hough Transform method.

Many pathologists use blood analysis with chemical process in diagnosing Malaria. Unfortunately, it is time consuming, requires blood analyst and can lead to false results. Though they brought a number of developed systems in accelerating the diagnosis this last decade, most of the automated diagnosis methods are deployed on 100X microscopes and more. The presented performance criteria are either one or a maximum of two on the four that are normally awaited, with an appreciation of a mean sensitivity at 92.22% calculated from [17]. The expensiveness of these previous systems is an actual condition in decision-making to health access for low-income countries. The author's aim is therefore to design a forceful process adapted to microscopic images of a different standard from the tropical sub-Saharan ecosystem for more efficiency, availability and financial reasons.

The work is thus organized in presenting the general methodology in section 2, dealing first with the blood smears preparation, the laboratory count of parasites, the image acquisition process. This, was followed by the presentation of two noteworthy methods designed for comparison with the same use constraints. Sections 3 unfolds respectively with the experimental results and discussion before the conclusion tails the paper in section 4.

2. METHODOLOGY OF WORK

2.1 Laboratory Analysis

We worked on blood collected from PMI Health Center Nkwen at Bamenda, Azire Preventive Hospital at Bamenda and District Hospital of Logbaba at Douala. Thin blood smears preparation is performed by using Giemsa coloration in conformity with the standard [26]. The laboratory count of parasite was carried out with the support of in-situ experts.

2.2 Image Acquisition Process

Images are captured in real time with an acquisition system comprising a binocular microscope, Type XSZ-107BN (No 002890), with 100X and 40X magnification; a webcam digital camera, type USB2.0 PC camera (SN9C203); and a computer Intel® Core™, 2 Duo processor T6500, 4GB DDR3 Memory, for images capture and processing. The link between computer and camera is provided by a USB interface and CyberLink YouCam 4 software drivers. The 100X regions of interest on 40X images are extracted proportionally according to the magnification ratio.

2.3 Conventional Approach

Moved by white and red blood cells counting method [23], the conventional approach unfolds the following steps namely image conversion from RGB to gray, median filtering, Gray thresholding, filling of holes, removal of borders, image labelling. The previous, implemented by author's care,

are completed with the cells form factor calculation, detection and counting of infected cells as described in § 2.4.3 for estimation of parasitemia.

2.4. Improved Method

This new approach follows the general synopsis of the conventional method where some new concepts are included on typical phases for innovation. The 2-stage adaptative median filtering (§ 2.4.1) and the Sauvola's segmentation (§ 2.4.2) are respectively put in place and computed at the preprocessing and the cells extraction steps. For cells classification (§ 2.4.3), the form factor is always estimated in order to detect and count infected cells.

2.4.1 Two-stage Adaptive Median Filter

The filter combines two concepts, both adaptative and contextual according to the literature sources. For the first, the size of our window is not fixed and the filtering is done once a specified condition is fulfilled [27]. For the second, we partitioned the pre-processing depending of the local disparity of information in the image [28]. The filtering algorithm is then summarized as follow:

1. Let $s_{max} \times s_{max}$ be the maximum window size and initialize *s=1*
   Let $I(i,j)$ be a window of size *s×s* centered at *(i, j)*, which means
   $I(i,j) = \{I(i+p, j+q), -s \leq p \leq s \; and \; -s \leq q \leq s\}$
2. Compute I_{mean}, I_{min}, I_{max} and I_{med} which are mean, minimum, maximum and median of the pixel values in $I(i,j)$ respectively
3. While $s < s_{max}$
4. Compute the negative median, the positive median, the negative gradient and the positive gradient of the pixel values in $I(i,j)$, respectively $I_{min}^{med}(i,j)$, $I_{max}^{med}(i,j)$, $I_{min}^{mean}(i,j)$ and $I_{max}^{mean}(i,j)$, by $I_k^l(i,j) = \left| I_l\ (i,j) - I_k\ (i,j) \right|$, with $l \sim med, mean$ and $k \sim min, max$
5. Compute the mean Me_k^l, the maximum Ma_k^l and the standard deviation Sd_k^l of I_k^l
6. Compute the fringing weighting coefficients K_k^l
$$K_k^l = \exp\left(-\frac{Me_k^l}{Sd_k^l}\frac{I_k^l}{Ma_k^l - I_k^l}\right)$$
7. Compute the index of fit $D_k^l = 1 - K_k^l$
8. * If $I_{min} + D_{min}^{med} < I_{med} < I_{max} - D_{max}^{med}$, then the median value is not an impulse, the algorithm goes to 9 to check if the current pixel is an impulse.
   * Else the size of the window is increased and 8 is repeated until the median value is not an impulse, then the algorithm goes to 9; Until the maximum window size is reached, in which case the median value is assigned as the filtered image pixel value I_{med}.
9. * If $I_{min} + D_{min}^{mean} < I < I_{max} - D_{max}^{mean}$, then the current pixel value is not an impulse, so the filtered image pixel is unchanged.
   * Else the image pixel is corrupted and can either equal to $I_{min} + D_{min}^{mean}$ or to $I_{max} - D_{max}^{mean}$, then the filtered imaged pixel is assigned the median value I_{med} from 2.

2.4.2 Image Segmentation

Global thresholding methods like optimal global thresholding typically fails when the background illumination is highly non uniform. one approach used to compensate for irregularities in illumination is the use of variable thresholding [29]. This approach computes a threshold value at every point (i,j) in the image, based on one or more specified properties of the pixels in the neighborhood. We illustrated the basic approach to local or variable thresholding using the local standard deviation and mean of the pixels in a neighborhood of every point in an image [30]. The local threshold of Sauvola is as follows:

$$T(i,j) = m(i,j)[1 + k_b\left(\frac{\delta(i,j)}{R} - 1\right)]$$

Where R is the maximum value of the standard deviation and k_b is a bias, which takes positive values in the range [0.2, 0.5]. In order to compute the threshold, the integral image of the input image is first extracted in each single pixel, the local mean $m(i,j)$ and the local variance $\delta^2(i,j)$ [31] are then computed.

2.4.3 Cells Classification

In order to distinguish between infected and non-infected red blood cells, we extracted features from the image array and computed new variables that concentrated information to separate classes. One set of features had been chosen for development, geometric shape features [32]: area, perimeter and form factor. The detection is finally achieved from the form factor values of cells which varies as the shape of an object varies. Moreover the form factor range of a malaria infected red blood cell is 1.26$\pm$ 0.14, 1.57$\pm$0.38 and 1.35$\pm$0.22 for respectively low, medium and high parasitemia [33].

3. EXPERIMENTAL RESULTS AND DISCUSSION

3.1 Data

After blood extraction, thin blood smears preparation with Giemsa coloring, laboratory count of parasites and acquisition process with the microscope, we produced a database of 100 original images of 100X and 40X magnifications, 50 each, with spatial resolutions 300x320 and 120x128 respectively and 8 digits in JPEG format. A set of the sample number 16 of both 100X (coded 10016 in figure 1a) and 40X (coded 4016 in figure 1b) magnification is presented in figure 1. The region of interest is defined by the 100X magnification image. It is acquired directly from the microscope with 100X magnification, where infected red blood cells are visibly located in the laboratory as it is indicated here by two arrows (figure 1a). It is then extracted from the acquired image from the microscope with 40X magnification. In this case, it is very challenging to identify the infected red blood cells in the laboratory (figure 1b) without testing an appropriate algorithm.

3.2 Results and Discussion

The conventional and new methods have been deployed simultaneously on the same database for the step by step comparison. The histograms portray the improvement due to the 2-stage median filtering. Moreover, the binary image obtained with classical approach has some cells stuck together and many are absent because of their obliteration as a result of a poor segmentation. The robustness of Sauvola segmentation method has led to an extraction of numerous cells therefore allowing a richer diagnosis. After classification and counting, the parasitemia are estimated and the results for both laboratory and automatic processes selected randomly are presented in table 1.

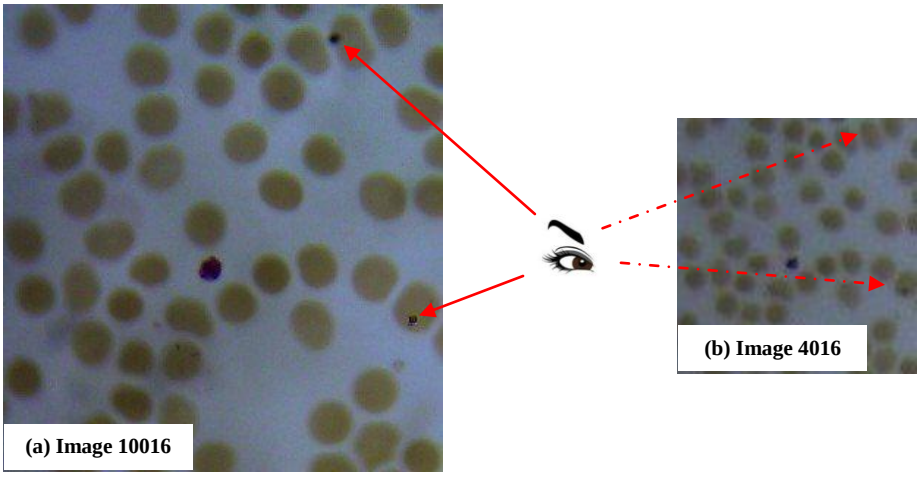

FIGURE 1: Original microscopic images of blood smears, serial number 16 both 100X (a) and 40X (b) magnifications.

40X magnification			Laboratory approach	100X magnification		
Image sample	Automatic approach			Image sample	Automatic approach	
	Classical	New			Classical	New
407	2.22	1.92	1.81	**1007**	2.08	4
4013	8.33	3.70	1.72	**10013**	4.76	7.69
4016	0	0	4.87	**10016**	5.55	4.76
4017	2.94	4.25	2.00	**10017**	2.17	2.08
4022	4.08	6.94	2.94	**10022**	7.01	8.69
4025	2.22	9.23	3.27	**10025**	11.53	16.36
4029	8.33	9.61	2.85	**10029**	10.52	17.54
4033	4.65	10.86	2.56	**10033**	15	10.86
4036	16.27	4.83	3.57	**10036**	9.25	2.43
4042	7.69	10	8.88	**10042**	8.69	8.69
4046	14.28	3.22	3.44	**10046**	10.41	12.96
4050	7.69	11.11	2.94	**10050**	11.53	6.66

TABLE 1: Parasitemia (in %) estimation results of laboratory and automatic (conventional and new) methods on both 40X and 100X magnification images.

Three major measurements expressed in terms of true positives (TP), false positives (FP), true negative (TN) and false negatives (FN), are used to evaluate the algorithm performances of the automatic methods for both 40X and 100X [34], especially sensitivity, specificity and accuracy (table 2).

Magnification range	Performance measurements		
	Designation	Conventional method	New method
100X	Sensitivity (%)	86.67	89.19
	Specificity (%)	93.46	95.25
	Accuracy (%)	93.19	95.10
40X	Sensitivity (%)	52.63	81.58
	Specificity (%)	97.65	97.11
	Accuracy (%)	95.67	96.71

TABLE 2: Performance results from the two methods according to the magnifications 100X and 40X.

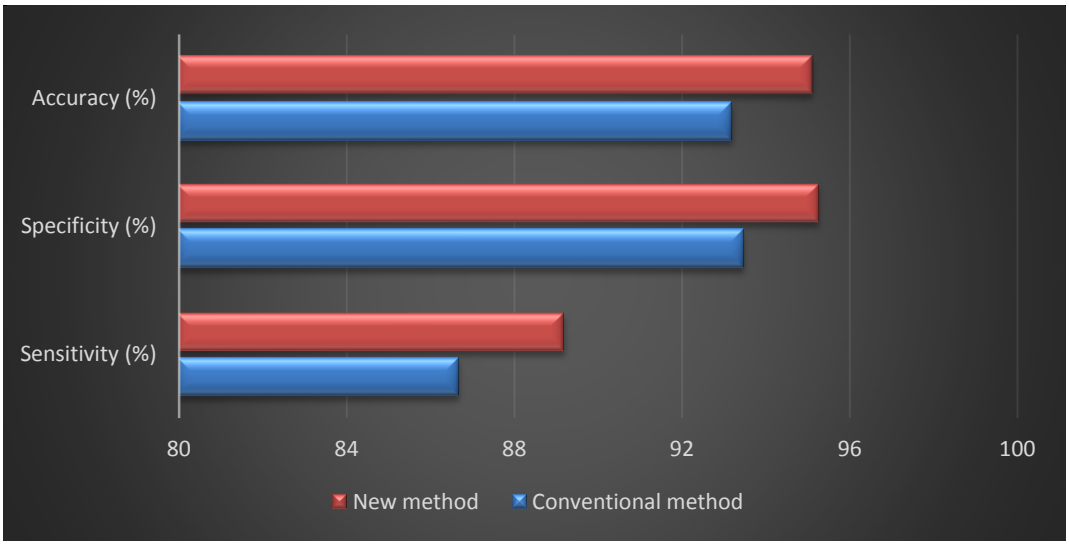

FIGURE 2: Comparison of performance criteria between on 100X between conventional and new methods.

With all performance criteria considered on 100X image tests (figure 2), the new method is above the conventional with at least 1.79%. The sensitivity classifies an individual as sick, so as to say, the greater its percentage, the more precise the diagnosis. With a difference of 2.52% in sensitivity between the two approaches, a serious demarcation is observed and makes therefore the improved method standing for a step forward towards the goals awaited. The use of the global thresholding in the conventional method contributed to the failure of cells detection in their individual consideration. This has been forcefully corrected with the help of Sauvola segmentation implemented in the new approach, leading therefore to the understanding of proper identification of diseased-free patients through the specificity percentage.

Though existing the inversed comportment between sensitivity and specificity values, the results are still valid and valuable in terms of equilibrium and a good conciliation of both criteria to the author's method, certainly due to the 2-stage median filter. An improvement of both performances is visible as well as their togetherness in the consideration of the robustness in the improved approach.

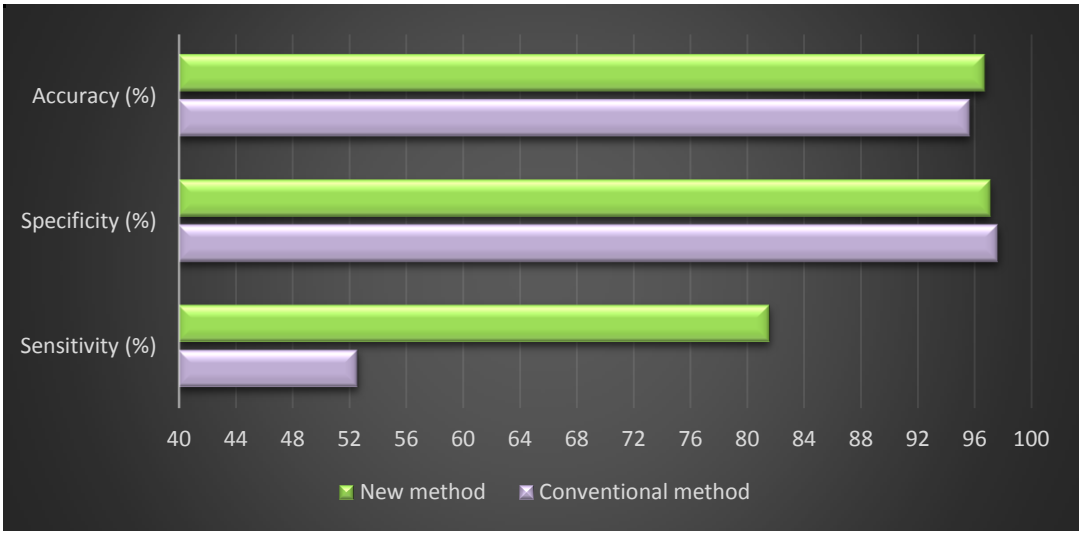

FIGURE 3: Comparison of performance criteria between on 40X between conventional and new methods.

A glance at the sensitivity shows on how the ability of the 40X test (figure 3), to correctly classify a patient as diseased, is well pronounced than the one of the conventional method. The conventional method produces successfully, at the highest percentage, a true negative when used in a non-infected population. With a negligible difference in specificity, our approach continues to faithfully convince in the diagnosis exercise. And so, the detection and the estimation of the parasitemia is well opened. Since the accuracy of the method involves at the same time the sensitivity and the specificity, the improved system globally performs at 40X. Therefore, an acute appreciation of the improved method allows the tests carried out on the patients to be valid and powerfully persuasive.

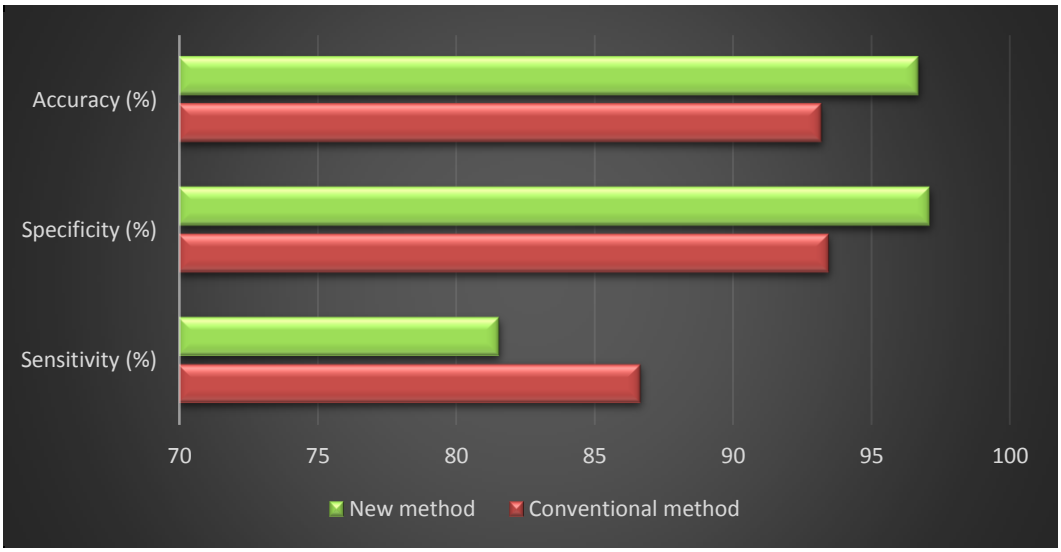

FIGURE 4: Comparison of performance criteria between 100X classical and 40X new.

With poor results observed on the performance criteria of the conventional method on 40X magnification, it appears clearly that the classical approach is not adapted for that magnification. On the contrary, the comparison of the conventional method in 100X and the new in 40X magnification, portrays that the performances of the improved system are challenging the classical one, with high difference and from two criteria (accuracy and specificity) over three, while the third (sensitivity) is maintained advanced in 100X. This is therefore opening a positive greater inquisition in the diagnosis with 40X magnification.

We then noticed that our results with the new approach are close to that obtained with automated detection of malarial pigment from a haematology analyser [16] and with quantitative buffy coat [10]. Concerning automated diagnosis of malaria, beyond the effect parameters related to the database (magnification range, size, sensor characteristics, …), the quality of the processing mainly depends on the relevancy of its flow chart, especially the preprocessing approach, the RBC segmentation method, the features extracted and the classification technique used. The authors have innovated on all these steps compared to the conventional method deployed.

The relative supremacy of the new approach performed on 40X magnification compared to the conventional applied on 100X, is an indication of its superiority on the understanding of most of literature results from the use of 100X. The new system keeps ahead in accuracy with a difference of 19.52% and 5.59% competed with *Yunda* [17] and *Pramit* [22] works respectively. The first is based on morphological gradient method, Agnes and K-Median, color features and textural, multilayer perception. Without considering the last step, the other approaches are very conventional to challenge our preprocessing and segmentation techniques. The second deals with Laplacian filtering on the 3 color components, global thresholding, minimal pixel intensity distance. The classifier looks not sufficiently sturdy to produce strong results.

The new algorithm also improves in specificity with 8.6%, 9.11%, 3.94% and 0.11%, respectively from *Das* [17], *Puwar* [17], *Savkare* [18] and *Maitethia* [20] techniques. The first is a compilation of gray world assumption, geometric mean filter, marker controlled watershed algorithm, 80 textural and 16 morphological features, SVM classifier. The technique is well elaborated but the great number of features should not always be a cause of efficiency. The second author combines local histogram equalization, energy minimization, pixel intensity, K-mean clustering. The third implemented the image smoothening and edge sharpening with the median and Laplacian filters, global Otsu thresholding, geometrical and color and statistical features, support vector machine for cell classification. The fourth algorithm combines means and median filtering, Otsu and Zack thresholding, texture and color features, Artificial Neural Network. The global thresholding has proved its limits on sensitive object detection. The authors think the choice of the two-stage adaptive median filter and the Sauvola thresholding have been appropriate for the closeness of the red blood cell segmentation. The use of the form factor as the unique feature for cell classification to achieve the process has also been very persuasive. It has reinforced the class of workmanship deployed in [33].

On 100X magnification range, the author's method generated a sensitivity almost equal to the content based image algorithms [21]. And so, whiles the preprocessing and segmentation steps are common, a final classification based on an interesting two-stage binary tree-classifier is used to fight the results back. The narrow variation of this sensitivity is increased with the Bayes Decision theory to build a two stage erythrocyte classifier based for measurement of malaria [23]. Fortunately, the sensitivity of 40X images is very promising according to that of 100X images for the conventional method and that of the mean value calculated from Razzak's works [17]. Specificity and accuracy outclass several results produced by the previous methods both on 40X and 100X magnification ranges [18,22]. Our execution time for 40X images is 48 seconds while that of 100X images is 344, meaning a reduction ratio of 86%. We finally gained more time and money with 40X magnification than with 100X since microscopes attributed to the first are cheaper than those to the second.

4. CONCLUSION

We have completed a conventional approach and proposed a new one for improvement for comparison on the common ground and optical bases. The works revealed that automation of malaria diagnosis is essential and possible by using a 40X microscope. The process becomes then cheap compared to the usual 100X microscope acquisition system in most medical centers. We have provided a reliable and efficient algorithm compared with some other previous works found in the same issues by image processing. The proposed algorithm performance is obviously improved in figures and in execution time. Our results are opening a thinking on a reconsideration about the coupling of accuracy of a method and cheapness of its implementation. This is therefore highlighting the possibility in automation of malaria diagnosis for low-income countries in most tropical and sub-tropical countries in Africa and America.

5. REFERENCES

[1] Arash Mehrjou, Tooraj Abbasian, Maziar Izadi. ''Automatic malaria diagnosis system.'' Robotics and Mechatronics (ICRoM), First RSI/ISM International Conference. Tehran, Iran, 2013.

[2] Elizabeth A. Ashley, Khin Maung Lwin, Rose McGready, Win Htay Simon, Lucy Phaiphun, Stephane Proux, Nantawan Wangsean, Walter Taylor, Kasia Stepniewska, Wimon Nawamaneerat, Kyaw Lay Thwai, Marion Barends, Wattana Leowattana, Piero Olliaro, Pratap Singhasivanon, Nicholas J. White and Francois Nosten. ''An open label randomized comparison of mefloquine– artesunate as separate tablets vs. a new co-formulated combination for the treatment of uncomplicated multidrug-resistant falciparum malaria in Thailand.'' Tropical Medicine and International Health – vol. 11 no 11, pp 1653 –1666, 2006.

[3] Stephen Y. Gbedema, Marcel T. Bayor, Kofi Annan, Colin W. Wright. ''Clerodane diterpenes from Polyalthia longifolia (Sonn) Thw. var. pendula: Potential antimalarial agents for drug

resistant Plasmodium falciparum infection.'' Journal of Ethnopharmacology 169, 176 – 182, 2015.

[4] Snow R.W. and Gilles H. M. ''The epidemiology of malaria - Essential malariology. 4th edition. London, New York, 2002.

[5] Saad H. Abdalla and Geoffrey Pasvol. ''Malaria: A Hematological Perspective.'' Tropical Medecine Science and Practice, Vol.4. Ed. Imperial College Faculty of Medicine, 2004,16 pgs.

[6] D. C. Warhurst, J. E. Williams. ''Laboratory diagnosis of malaria.'' Journal of Clinical Pathology (J Clin Pathol) Vol.49, pp 533-538, 1996.

[7] Janet Cox-Singh, Timothy M. E. Davis, Kim-Sung Lee, Sunita S. G. Shamsul, Asmad Matusop, Shanmuga Ratnam, Hasan A. Rahman, David J. Conway, and Balbir Singh. ''Plasmodium knowlesi malaria in humans is widely distributed and potentially life threatening. Clinical Infectious Diseases.'' Vol. 46 (2), pp165–171, 2008.

[8] World Health Organization. World Malaria Report. WHO Global Malaria Programme. World Health Organization, Geneva, Meeting of 11 - 13 Sept. 2013.

[9] Christophe Antonio-Nkondjio, Jean Atangana, Cyrille Ndo, Parfait Awono-Ambene, Etienne Fondjo, Didier Fontenille, Frederic Simard. ''Malaria transmission and rice cultivation in Lagdo, northern Cameroon.'' Transactions of the Royal Society of Tropical Medecine and Hygiene 102, 352 – 359, 2008.

[10] Chotivanich K., Silamut K. and Day, N. P. J. ''Laboratory diagnosis of malaria infection- A short review of methods.'' New Zealand Journal of Medical Laboratory Science, vol. 61, pp. 4-7, 2007.

[11] M.T. Makler, R.C Piper, W.K Milhous. ''Lactate Dehydrogenase and the Diagnosis of Malaria.'' Elsevier Journal, Parasitology International, Vol. 14, Issue 9: pp 376–377, 1998.

[12] G.O. Adeoye, I.C. Nga. ''Comparison of Quantitative Buffy Coat technique (QBC) with Giemsa-stained thick film (GTF) for diagnosis of malaria.'' Elsevier Journal, Parasitology International, Vol. 56, Issue 4: pp 308–312, 2007.

[13] Clendennen, T.E., Long, G.W. and Baird, K. J. ''QBC and Giemsa stained thick blood films: diagnostic performance of laboratory technologists.'' Trans. R. Soc. Trop. Med. Hyg., vol. 89, issue 2: pp 183–184, 1995.

[14] Anthony Moody. ''Rapid Diagnostic Tests for Malaria Parasites.'' Clinical Microbiology Review. Vol. 15 no.1: pp 66-78, 2002.

[15] Hanscheid T., Melo-Cristino J. and Pinto, B. G. ''Automated detection of malaria pigment in white blood cells for the diagnosis of malaria in Portugal.'' American Journal of Tropical Medicine and Hygiene, vol. 64: issue 5, pp. 290-292, 2001.

[16] C. Fourcade, M. J. C. Casbas, H. Belaouni, J. J. D. Gonzalez, P. J. J. Garcia, M. A. E. Pepio. ''Automated detection of malaria by means of the haematology analyser Coulter® GEN.STM.'' International Journal of Laboratory Hematology, Clinical & Laboratory Haematology, Vol. 26: Issue 6, pp 367–372, 2004.

[17] M. I. Razzak. ''Automatic Detection and Classification of Malarial Parasite.'' International Journal of Biometrics and Bioinformatics (IJBB), Vol.9: Issue 1, pp 1-12, 2015.

[18] S. S. Savkare, S. P. Narote. ‘‘Automatic Detection of Malaria Parasites for Estimating Parasitemia.’’ International Journal of Computer Science and Security (IJCSS), Vol.5: pp 310-315, 2011.

[19] Pranati Rakshi and Kriti Bhowmik. ‘‘Detection of presence of Parasites in Human RBC In Case of Diagnosing Malaria Using Image Processing.’’ Proceedings of the 2013 IEEE Second International Conference on Image Information Processing (ICIIP-2013), 2013.

[20] Daniel Maitethia. ‘‘A rapid malaria diagnostic method based on automatic detection and classification of plasmodium parasites in stained thin blood smear images “, M.Sc. Thesis, the University of Nairobi, Kenya, 2014.

[21] Mohammad Imroze Khan, Bhibhudendra Acharya, Bikesh Kumar Singh, Jigyasa Soni. ‘‘Content Based Image Retrieval Approaches for Detection of Malarial Parasite in Blood Images.’’ International Journal of Biometrics and Bioinformatics (IJBB), Vol. 5: Issue 2: pp 97-110, 2011.

[22] Pramit Ghosh, Debotosh Bhattacharjee, Mita Nasipuri, Dipak Kumar Basu. ‘‘Medical Aid for Automatic Detection of Malaria.’’ Communications in Computer and Information Science (CCIS), Vol. 245, pp 170-178, 2002.

[23] Dian Anggraini, Anto Satriyo Nugroho, Christian Pratama, Ismail Ekoprayitno Rozi, Vitria Pragesjvara, Made Gunawan. ‘‘Automated Status Identification of Microscopic Images Obtained from Malaria Thin Blood Smears using Bayes Decision: A study case in Plasmodium Falciparum.’’ Proceedings of International Conference on Advanced Computer Science & Information Systems, Bandung, Indonesia, 2011.

[24] Pooja R. Patil, G. S. Sable, Gauri Anandgaonnkar. ‘‘Counting of WBCs and RBCs from blood images using gray thresholding.’’ International Journal of Research in Engineering and Technology (IJRET), Vol. 3, Issue 4: pp 391-395, 2014.

[25] Pawan Agrawal, Pradipti Verma. ‘‘Automated Detection and Counting of Red Blood Cell using image processing techniques.’’ International Journal of Scientific Research and Management (IJSRM) Vol. 3 Issue 4: pp 2692-2695, 2015.

[26] World Health Organization. Bench Aids for the diagnosis of Malaria infections. WHO Global Malaria Programme, Geneva, Switzerland, 24 pgs, 2000.

[27] Mamta Juneja and Rajni Mohana. ‘‘An Improved Adaptive Median Filtering Method for Impulse Noise Detection.’’ International Journal of Recent Trends in Engineering. Vol.1(1): pp 274-278, 2009.

[28] Thomas F. N. Kanaa, E. Tonye, G. Mercier, V. Onana. ‘‘Détection des nappes d’hydrocarbures dans les images RSO par morphologie mathématique.’’ Teledetection, vol.3, pp 215-229, 2004.

[29] Rafael C. Gonzalez, Richard E. Woods and Steven L. Eddins (2009). Digital Image Processing Using MATLAB, 2nd Edition. Gatesmark Publishing LLC.

[30] O. Imocha Singh, Tejmani Sinam, O. James and T. Romen Singh. ‘‘Local Contrast and Mean based Thresholding Technique in Image Binarization.’’ International Journal of Computer Applications (0975 – 8887) Vol.51, No.6, 2012.

[31] Faisal Shafait, Daniel Keysers and Thomas M. Breuel. ‘‘Efficient Implementation of Local Adaptive Thresholding Techniques Using Integral Images.’’ Conference Proceedings SPIE, Vol. 6815, 681510, 2008.

[32] Abdelrahman A. & Abdallah A. ‘‘Signature verification system based on support vector machine classifier.’’ the international arab conference on information technology (acit’2013), 2013.

[33] R. Renuka Devi, V. Rajagopal, M. Senthil Kumar and G. Magesh. ‘‘Computerized Shape Analysis Of Erythrocytes And Their Formed Aggregates In Patients Infected With P. Vivax Malaria.’’ Advanced Computing: An International Journal (ACIJ), Vol.2, No.2, pp71-77, 2011.

[34] Milan Sonka, J. Michael Fitzpatrick. ‘‘Handbook of Medical Imaging - Medical Image Processing and Analysis.’’ Volume 2. Bellingham, Washington: SPIE Press, USA, 2009.